ADVANCED INTELLIGENT SYSTEMS
www.advintellsyst.com

Multi-Field Synergy Manipulating Soft Polymeric Hydrogel Transformers

Dachuan Zhang, Jiawei Zhang, Yukun Jian, Baoyi Wu, Huizhen Yan, Huanhuan Lu, Shuxin Wei, Si Wu,* Qunji Xue, and Tao Chen**

Transformers are imaginary hard robots that could deform into various shapes according to external circumstances, and the development of intelligent soft Transformers is of great interest. Herein, novel remotely controlled soft Transformers based on a shape memory hydrogel system is proposed. The hydrogel is obtained by embedding Fe_3O_4 magnetic nanoparticles into a poly(*N*-(2-hydroxyethyl) acrylamide)-gelatin double network structure. The reversible coil-triple-helix transformation of gelatin renders the hydrogel with shape memory and self-healing behaviors. The introduction of Fe_3O_4 nanoparticles provides both photothermal heating and magnetic manipulation functions. The hydrogel can deform on navigation in a magnetic field, and the deformed shape can be fixed and shape recovery can also be accomplished with the assistance of light irradiation. Taking advantage of the magnetically driven actuation and light-assisted shape memory, remotely controlled shape memory process can be accomplished. Moreover, a series of soft robots, including hydrogel athlete which can do sit-ups, hydrogel Transformers that can deform and navigate through a maze, hydrogel space station and hydrogel spacecraft that can be docked in the air, are fabricated. This work will inspire the design and fabrication of novel smart polymer systems with synergistic functions.

1. Introduction

Transformers are imaginary hard robots that has unique ability to transfer into various shapes including vehicles (**Figure 1**a); it is anticipated that the development of soft Transformers is of great interest in both fundamental research and application fields. As one kind of emerging smart materials, shape memory polymers (SMPs), which can fix temporary shapes and recover to original shapes under external stimuli,[1–4] have attracted increasing interest and shown potential applications in many fields including biomedical, textile, flexible electronics, data encryption, and so on,[5–8] which render them as promising candidates to fabricate soft Transformers. Traditional SMPs are thermo-activated elastomers, and the temporary shapes are fixed by vitrification or crystallization of polymer chains.[9,10] With the development of intelligent polymeric materials, shape memory hydrogels (SMHs),[4,11,12] have received intensive attention. By introducing reversible switches that include hydrogen bonds,[13–15] host–guest recognition,[16,17] metal–ligand coordination,[18,19] etc., SMHs can respond to many stimuli such as light,[3,20–22] heat,[21,23–25] chemical,[24,26–28] ultrasound,[29] electric field,[30] and so on. However, there are still many limitations, for example, the temporary shapes of traditional SMPs and novel SMHs are often generated manually, and in the shape memory process, especially for SMHs, it is indispensable need to

D. Zhang, Prof. J. Zhang, Y. Jian, B. Wu, H. Yan, H. Lu, S. Wei, Prof. Q. Xue, Prof. T. Chen
Key Laboratory of Marine Materials and Related Technologies
Zhejiang Key Laboratory of Marine Materials and Protective Technologies
Ningbo Institute of Material Technology and Engineering
Chinese Academy of Sciences
Ningbo 315201, China
E-mail: zhangjiawei@nimte.ac.cn; tao.chen@nimte.ac.cn

D. Zhang
Nano Science and Technology Institute
University of Science and Technology of China
No. 166 Renai Road, Suzhou 215000, China

Prof. J. Zhang, Y. Jian, B. Wu, H. Yan, H. Lu, S. Wei, Prof. Q. Xue, Prof. T. Chen
School of Chemical Sciences
University of Chinese Academy of Sciences
19A Yuquan Road, Beijing 100049, China

Prof. S. Wu
Department of Polymer Science and Engineering
University of Science and Technology of China
No. 96 Jinzhai Road, Hefei 230026, China
E-mail: siwu@ustc.edu.cn

The ORCID identification number(s) for the author(s) of this article can be found under https://doi.org/10.1002/aisy.202000208.

DOI: 10.1002/aisy.202000208

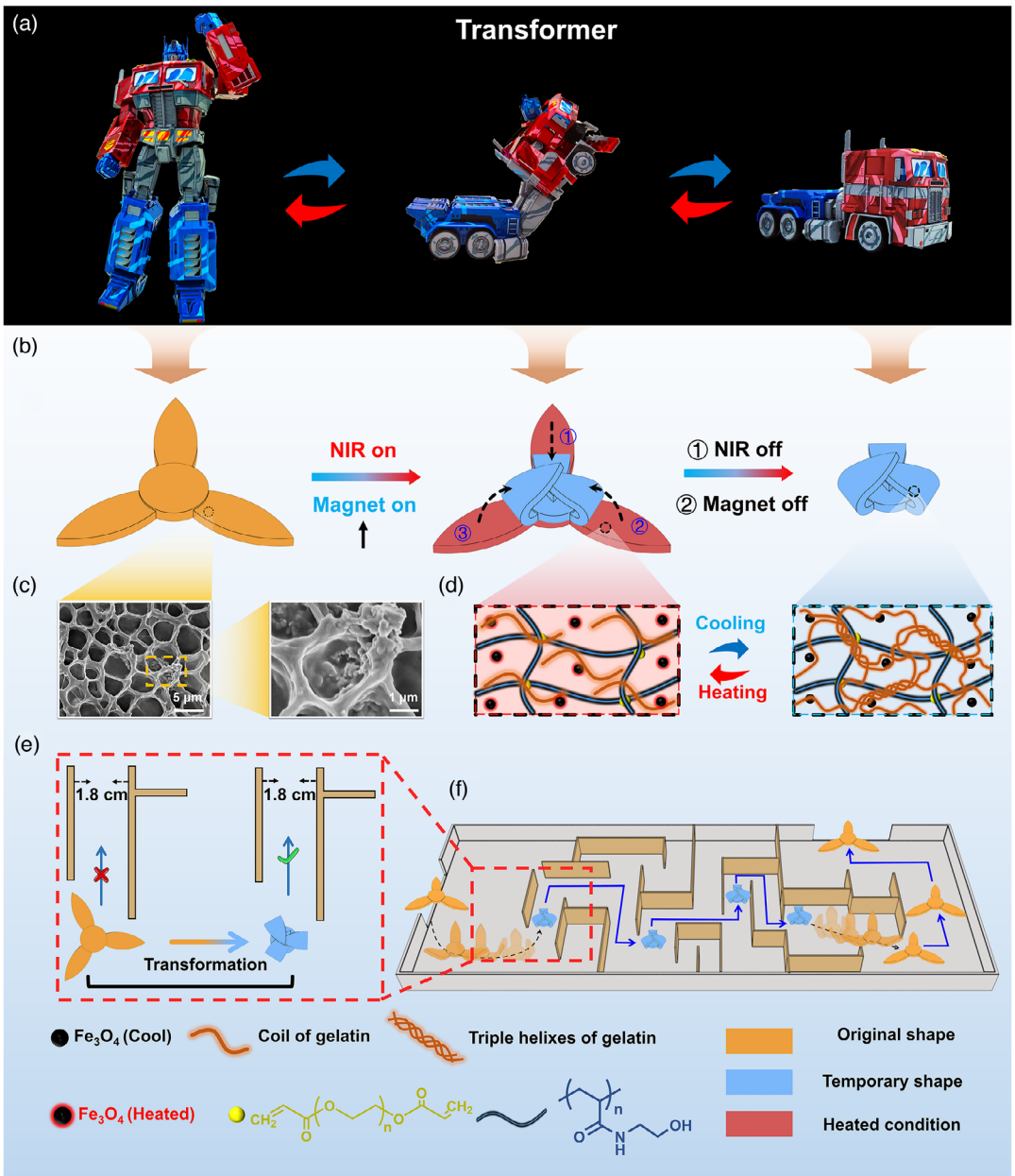

Figure 1. a) Images showing the shape transformation of a Transformer. b) The shape transformation process of a soft hydrogel Transformer under the coupling of magnetic field and NIR. c)The SEM images of HG-Fe_3O_4 hydrogel. d) The schematic illustration of the transition of gelatin between coil and triple-helix structure. e) The soft Transformer can cross the narrow notches after shape morphing. f) The soft Transformer first deforms into a folded shape, then passes through the narrow passages of the special maze, and finally recovers to the original shape in a wide area.

transfer the materials from one environment to another, which will restrain the potential applications of SMPs significantly.

Currently, novel methods that can manipulate the shapes of shape memory materials remotely are highly desired. A few attempts have been made to introduce actuating behavior in SMPs. For instance, Zhuo and co-workers have reported shape memory polyurethanes that are able to deform under UV light, fix the deformed shape in visible light, and recover to the original shape by heating.[20] In our previous work, a thermo-responsive actuating hydrogel layer and a pH-responsive memorizing hydrogel layer are combined to achieve a self-deformed shape memory behavior; the obtained bilayer hydrogel could deform in warm water and the shape fixation and shape recovery processes are realized via tuning the pH of the aqueous environment.[31] Moreover, several photothermal conversion material including gold nanorods,[32] carbon black,[33] and graphene oxide[34] have been introduced into thermo-responsive SMPs to trigger the shape recovery process by light. In addition to the aforementioned methods, to achieve remotely controlled shape memory process, magnetic nanoparticles[35–37] have been

considered as an effective additive to introduce noncontact actuation process.

Herein, we report novel photothermally and magnetically controlled SMH Transformers with untethered noncontact shape manipulation and directional navigation properties (Figure 1b). As shown in Figure S1, Supporting Information, a double network structure with a chemically crosslinked poly(*N*-(2-hydroxyethyl) acrylamide) (PHEAA) and a reversibly cross-linked gelatin network is prepared. There are a large number of hydrogen bonds between the gelatin chains; with temperature changing, hydrogen bonds are constantly broken and reformed, causing gelatin rapidly transition between coil and triple helix structure (Figure 1d).[38,39] Taking advantage of the reversible transition of gelatin, thermo-responsive shape memory performance and self-healing ability can be achieved. Moreover, Fe_3O_4 magnetic nanoparticles (Figure S2, Supporting Information) are introduced to endow the hydrogel with photothermal heating and magnetic manipulation properties. The morphology of the Fe_3O_4 involving double network hydrogel (HG-Fe_3O_4) was explored by scanning electron microscopy. The hydrogel shows typical porous structures with embedded nanoparticles, which indicates Fe_3O_4 nanoparticles have been successfully included into the hydrogel network (Figure 1c). As shown in Figure 1b, when the hydrogel is illuminated by near-infrared light (NIR), Fe_3O_4 nanoparticles will continuously convert light into heat, causing the hydrogel to be heated. As the temperature rises, the triple-helix structure of gelatin will untwist to single coils, which will lead to the decline of mechanical properties of the hydrogel. Thus, the hydrogel is easier to be pulled up by a magnetic field. As the temperature decreases, the triple-helix structure entangle again to fix the deformed shape. The fixed shape does not collapse even if the magnetic field is removed. When NIR is applied to the hydrogel again, the gelatin network undergoes a reversible transformation from triple helix to single coils, which promotes the shape recovery process. Combining the magnetic-field generated shape deformation and navigation, and the light-induced shape fixation and recovery, noncontact shape manipulation could be accomplished. Therefore, the obtained nanocompostie hydrogel could be applied as freely movable soft robots. As shown in Figure 1e,f, a three-pawed robot could be transformed and stabilzied into a smaller folded shape with the asstiance of NIR light and magetic field, then the folded robot could navigate across the narrow channels of a maze under the guidance of magectic field, and finally, it could recover to the original state. Our strategy may promote the development of novel SMH systems with various applications such as untethered soft robots.

2. Results and Discussion

2.1. Shape Memory Property

For a SMH, whether the temporary shape can be memorized stably and the original shape can recover perfectly under stimulus is important (**Figure 2**a). The shape memory property of the HG hydrogels were evaluated by bending tests. A strip-shaped sample was immersed in 60 °C water for 30 s to induce the disaggregation of the triple helixes of gelation, and the hydrogel will become soft. Then it was deformed to a circular shape and transferred into 5 °C water, and the temporary shape will be fixed because of the formation of gelatin triple helixes. The shape recovery behavior was further observed by immersing hydrogels in 60 °C water again. The shape fixity ratio (R_f) and shape recovery ratio (R_r) were defined by the following equations[40,41] (Figure S3, Supporting Information).

$$R_f = \frac{\theta_t}{\theta_d} \times 100\% \tag{1}$$

$$R_\gamma = \frac{\theta_d - \theta_f}{\theta_d} \times 100\% \tag{2}$$

where θ_d is the deformed angle, θ_t is the temporarily fixed angle, and θ_f is the final angle.

In this work, there are three factors that may affect the shape memory performance of the HG hydrogel: the degree of crosslinking (DCL), the amount of HEAA monomer and gelatin. Therefore, a series of controlled experiments were performed to verify the influence of these three factors. As shown in Figure 2b and Figure S4, Supporting Information, when the DCL, Supporting Information, is 3%, the hydrogel exhibits the best shape memory performance, and the shape fixation ratio and shape recovery ratio reach 89.3% and 89.7%, respectively. Then the effect of monomer content on the shape memory property was investigated. Figure 2c and Figure S5, Supporting Information, show that the optimal content of HEAA is 15 wt%, with R_r and R_f reach 89.3% and 89.7%, respectively. As the shape memory function of the hydrogel is derived from gelatin, the content of gelatin will be the most important factor to affect the shape memory performance. With the content of gelatin increasing, the shape fixation ratio and shape recovery ratio also increase; however,when the content of gelatin reaches 20 wt%, it is difficult to completely remove the bubbles from the prepolymer solution. So hydrogel with 15 wt% gelatin was chosen as the best result, with R_r and R_f reach 88.7% and 90%, respectively (Figure 2d, Figure S6, Supporting Information). It is worth noting that the hydrogel will not exhibit shape memory performance if the content of gelatin is too low (1 wt%). Furthermore, we test the cycled property of the shape memory effect of the hydrogel. It is found that the hydrogel still has good shape memory property after 10 cycles of testing. In other word, the gelatin chain do not lose the the property of coil-triple-helix transition after 10 cycles of testing. (Figure S7, Supporting Information)

The form of some plants in nature will alter with the change in external environments. For example, some flowers will bloom with the external temperature rising. The HG hydrogel we fabricated is a thermal-activated SMH. Once the temperature reaches the thermal transition temperature, the physical network of gelatin will collapse because the triple-helixes of gelatin will be untwisted to single coils. As shown in Figure 2e, the speed that the hydrogel recovers to its original shape is related to temperature. The higher the temperature, the shorter the recovery time is required. A hydrogel flower was designed to mimic the bloom of lotus. The petals of the flower were deformed in water at 60 °C and fixed to a flower bud shape at 5 °C. Then the bud was placed on a torus and transferred to water of 40 °C. Within 30 s, the

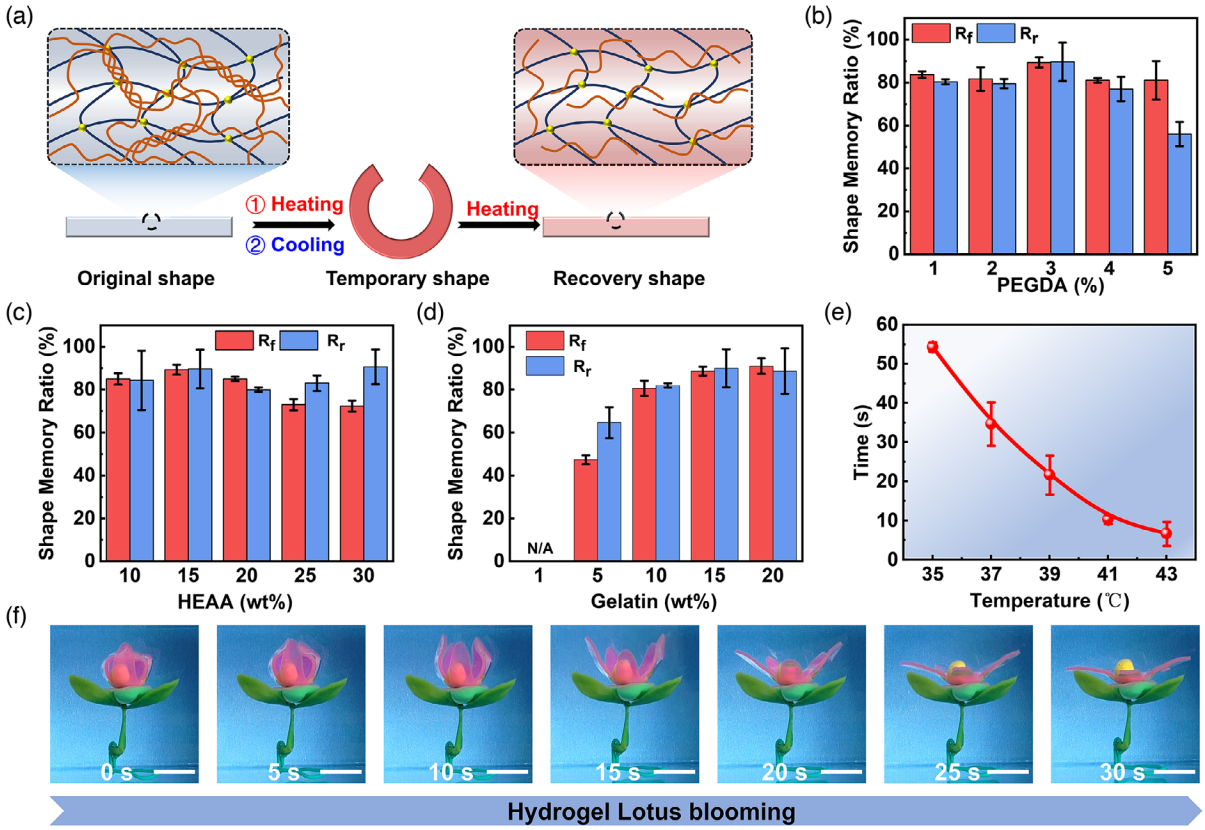

Figure 2. a) Illustration of the thermal-activated shape memory mechanism. b) The shape memory ratios as a function of the concentration of poly(ethylene glycol) diacrylate (PEGDA). (R_f and R_r are shape fixity ratio and shape recovery ratio, respectively). c) The shape memory ratios as a function of the concentration of HEAA. d) The shape memory ratios as a function of the concentration of gelatin. e) The shape recovery time as a function of temperature. f) Images showing the blooming process of a hydrogel Lotus. Scale bars: 2 cm.

hydrogel lotus will bloom perfectly (Figure 2f, Movie S1, Supporting Information).

2.2. Photo-Activated Self-Healing Ability

To endue the HG hydrogel with more fantastic properties, Fe_3O_4 magnetic nanoparticles were introduced in the hydrogel network to obtain HG-Fe_3O_4 hydrogel. The mechanical properties of the materials will be effectively improved by embedding of Fe_3O_4 nanoparticles; the maximum tensile stress and strain of HG-Fe_3O_4 hydrogel can reach 274 kPa and 120%, respectively (Figure S8, Supporting Information). The difference in mechanical properties among the three hydrogels can also be proved by rheological experiments in Figure S9, Supporting Information. It can be seen that G' and G'' of the HG-Fe_3O_4 hydrogel are higher than that of the H and HG hydrogel in the entire frequency range (0.1–100 rad s^{-1}) at 25 °C. In addition, rheological tests were performed at 25 and 40 °C. The results show that G' and G'' of the H hydrogel are almost unchanged (Figure S10, Supporting Information), while the modulus of HG-Fe_3O_4 hydrogel and HG hydrogel at 40 °C are significantly less than that at 25 °C (**Figure 3**a and Figure S11, Supporting Information), which indicate that the shape memory function is determined by the melting and gelation of gelatin.

As Fe_3O_4 nanoparticles could absorb and convert light to heat, the temperature of the HG-Fe_3O_4 hydrogel would increase with the irridiation of light. As shown in Figure 3b,c, Figure S12, S13, Supporting Information, pure HG hydrogel is illuminated by NIR (Energy density is 1.019 w cm^{-2}) for 300 s and the increase in temperature is negligible. As a comparison, the temperature of HG-Fe_3O_4 hydrogel with 1 wt% Fe_3O_4 increases to nearly 80 °C. In less than 30 s, the temperature can reach the melting temperature of gelatin. The content of Fe_3O_4 nanoparticles will also affect the speed and degree of heating. Even if the content of the embedded Fe_3O_4 is reduced to 0.1 wt%, the temperature of hydrogel also can be raised to 46 °C within 300 s.

As gelatin is a reversible physical crosslinking network with thermal-activated self-healing property,[42] after the introduction of light-to-heat conversion materials, photo-activated self-healing ability can be achieved. As shown in Figure 3e, the hydrogel is first destroyed, and both the PHEAA and gelatin networks will be damaged. The damaged hydrogels are then illuminated under light, which cause the gelatin network at the incision to melt. After switching off the light and cooling down, the single coil of gelatin at the incision will be tangled into triple-helix structure again, so the two hydrogels healed together. As shown in Figure S14, Supporting Information, a strip of HG-Fe_3O_4 hydrogel was cut at the middle and healed under NIR. After healing,

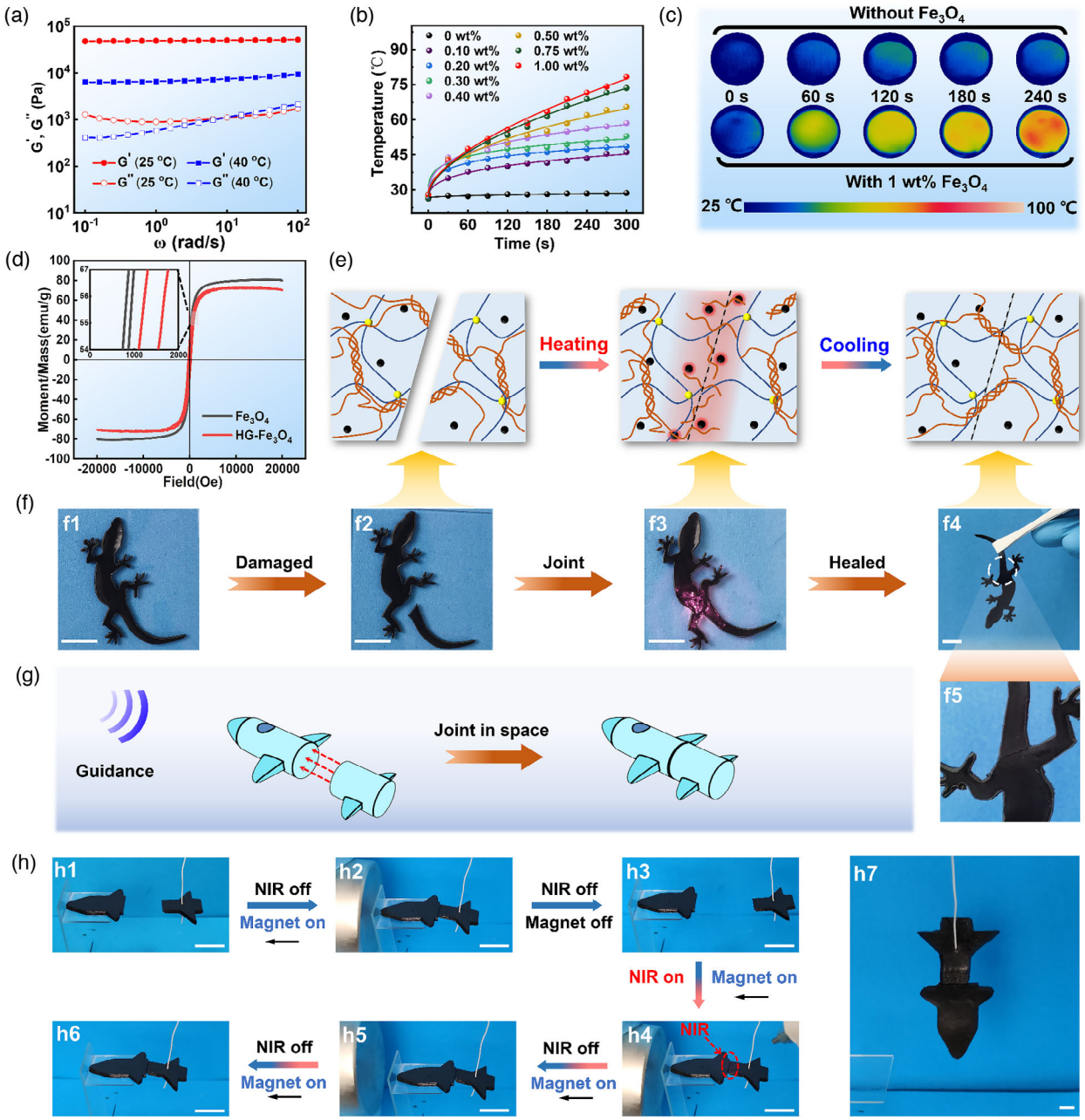

Figure 3. a) Frequency sweep data of HG-Fe_3O_4 hydrogel in terms of G′ and G″ at 25 °C and 40 °C. b) The temperature increase of the HG-Fe_3O_4 hydrogel with different mass ratio of Fe_3O_4 (0 wt% to 1 wt%) when irradiated by NIR from 0 to 300 s. c) The infrared images of the HG-Fe_3O_4 hydrogel with 0 wt% and 1 wt% Fe_3O_4 when irradiated by NIR for 0, 60, 120, 180, 240 s. d) The magnetic hysteresis curve of Fe_3O_4 nanoparticles and HG-Fe3O4 hydrogel. e) Schematic illustration of the self-healing mechanism. f) A gecko's broken tail repair process. g) Schematic illustration of a spacecraft joining with a space station in air. h) A hydrogel spacecraft would approach a hydrogel space station under the guidance of magnetic field, and the two parts would connect together under the assistance of NIR. Scale bars: 2 cm.

it could be stretched almost the same as the original hydrogel strip. Even HG-Fe_3O_4 hydrogel and HG hydrogel can be connected together by self-healing property (Figure S15, Supporting Information). As we all known, when a gecko senses danger, it will abandon its tail to mislead the enemy and escape. Inspired by this, a hydrogel gecko was prepared, and the broken tail could be reconnected with the body with the irradiation of light, and the healed gecko could be lifted up without breaking of the tail (Figure 3f, Movie S2, Supporting Information).

As the magnetic properties of the magnetic materials are critical to ensure their applications, the magnetic hysteresis loops (Figure 3d) of the Fe_3O_4 nanoparticles and HG-Fe_3O_4 hydrogel were measured at room temperature (25 °C) in an applied magnetic field of up to 20 000 Oe, and the HG-Fe_3O_4 hydrogel

exhibits superparamagnetic behavior. For the common self-healing process, the repaired parts usually need to be placed together manually; otherwise, the materials cannot be healed. With the addition of Fe_3O_4 nanoparticles, the HG-Fe_3O_4 hydrogel could be attracted by a permanent magnet (Figure S16, Supporting Information), the self-healing could happen in an unexpected way. As shown in Figure 3g,h and Movie S3, Supporting Information, a HG-Fe_3O_4 hydrogel space station is placed on a shelf, and a hydrogel spacecraft could approach the space station under the control of magnetic field, then NIR is applied to irradiate the connect parts; the spacecraft would dock with the space station because of the helix-coil transition of gelatin, realizing connection and self-healing in air.

2.3. Shape Recovery Induced by Photothermal Effect

For the HG hydrogel without Fe_3O_4 nanoparticles, the process of shape recovery only can be achieved in medium at a certain temperature, which will limit the application of SMHs greatly. With the addtion of Fe_3O_4 nanoparticles, when the hydrogel is illuminated by light, the embedded Fe_3O_4 nanoparticles will covert light into heat; therefore, the shape recovery process could be performed in air on the basis of photothermal effect.

As shown in Figure S17 and Movie S4, Supporting Information, a strip of HG-Fe_3O_4 hydrogel was deformed and fixed in a spiral shape in advance. To recover to original shape, the twisted portion is illuminated sequentially. In the beginning, a certain time is required for the hydrogel to increase its temperature to the melting point of gelatin, and the shape recovery speed is slow at this stage. With continuous light irradiation, the shape recovery speed would gradually increase until the hydrogel returns to the original shape. In Figure 3c, we have shown that the content of Fe_3O_4 nanoparticles will affect the heating speed of the hydrogel and the temperature eventually. As shown in **Figure 4**a, the HG-Fe_3O_4 hydrogel with a higher content of Fe_3O_4 requires shorter time to rise to 40 °C. Therefore, we designed a sequential shape-transformation Transformer whose petals can bloom in sequence. First of all, six petal-shaped HG-Fe_3O_4 hydrogels with different contents of Fe_3O_4 nanoparticles (two 1 wt%, two 0.3 wt%, and two 0.1 wt%) and two disc-shaped HG-Fe_3O_4 hydrogels (with 1 wt% Fe_3O_4) are assembled together utilizing self-healing ability (Figure 4b). The deformed and fixed shape are shown in Figure 4c. After illuminated by NIR, two HG-Fe_3O_4 (1 wt%) petals hydrogel flower would bloom first within 80 s, and next two HG-Fe_3O_4 (0.3 wt%) petals would bloom within 90 s. Finally, all

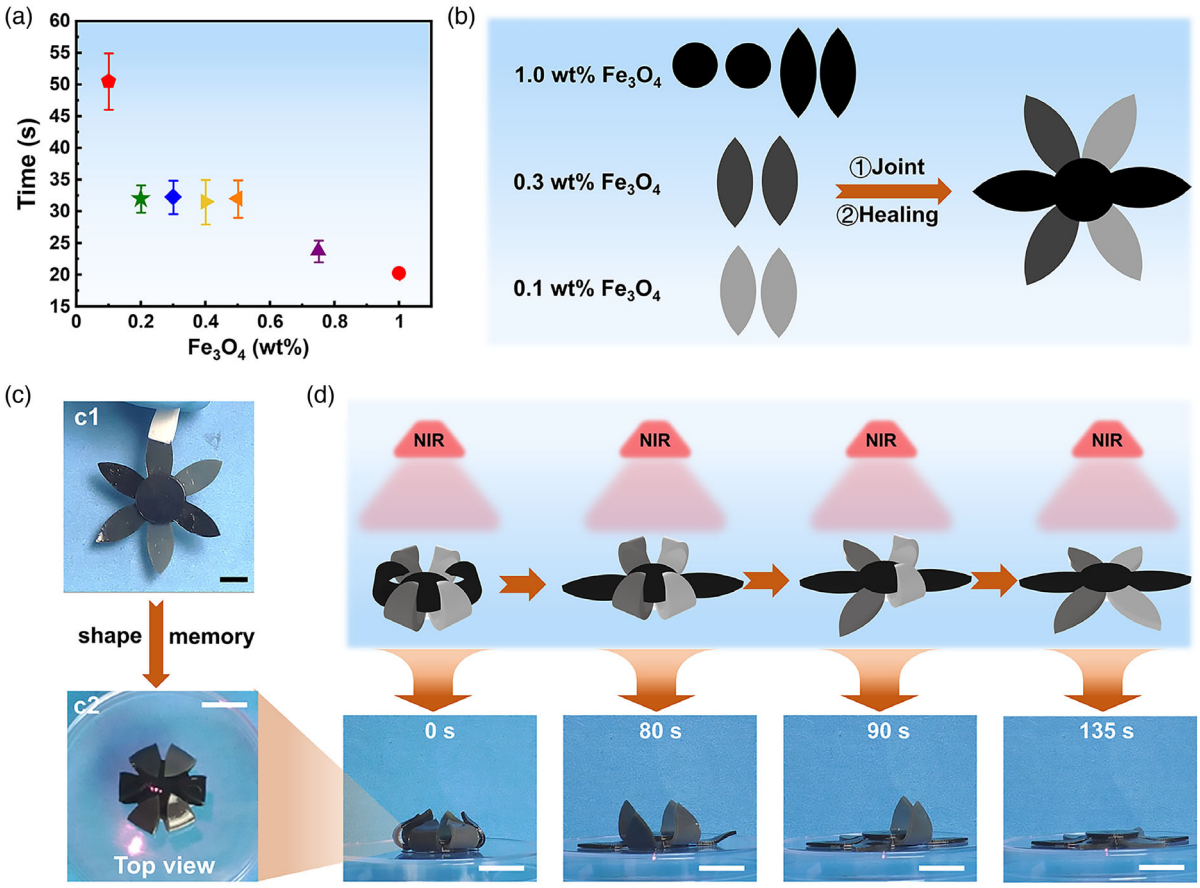

Figure 4. The sequential shape-transformation Transformer. a) The time of HG-Fe_3O_4 hydrogels with different content of Fe_3O_4 (0.1, 0.2, 0.3, 0.4, 0.5, 0.75, 1 wt%) require to reach 40°C under the irradiation of NIR. b) Schematic illustration of the assembly process of sequential shape-transformation Transformer. c) The top views of the original shape and temporary shape of the assembly hydrogel Transformer. d) The schematic illustration and images of the sequential shape-transformation process. Scale bars: 1 cm.

petals would bloom completely. (Figure 4d and Movie S5, Supporting Information).

2.4. Remotely Controlled Shape Memory Process

For traditional SMHs, the deformed shapes are often created by external force with direct contact. As the HG- Fe_3O_4 hydrogel could be attracted by a permanent magnet, combining with the photo-activated shape recovery property mentioned earlier, remotely controlled shape memory recovery cycles could be realized. As shown in **Figure 5**a, under the irradiation of light, the Fe_3O_4 nanoparticles continuously convert light to heat and transfer the heat to gelatin network, causing the melting of gelatin. As a result, the hydrogel becomes so soft that it is easier to be lifted up by a magnet. Keeping the magnet still and switching off the infrared light, the gelatin in the HG-Fe_3O_4 hydrogel will form triple-helix structure again as the temperature decreases, thus the temporary shape could be fixed. After switching the light on again, the hydrogel softens again and returns to the original shape.

A shape-transition robot that facilitated the deformation from 2D to 3D is constructed. There are two modes depending on

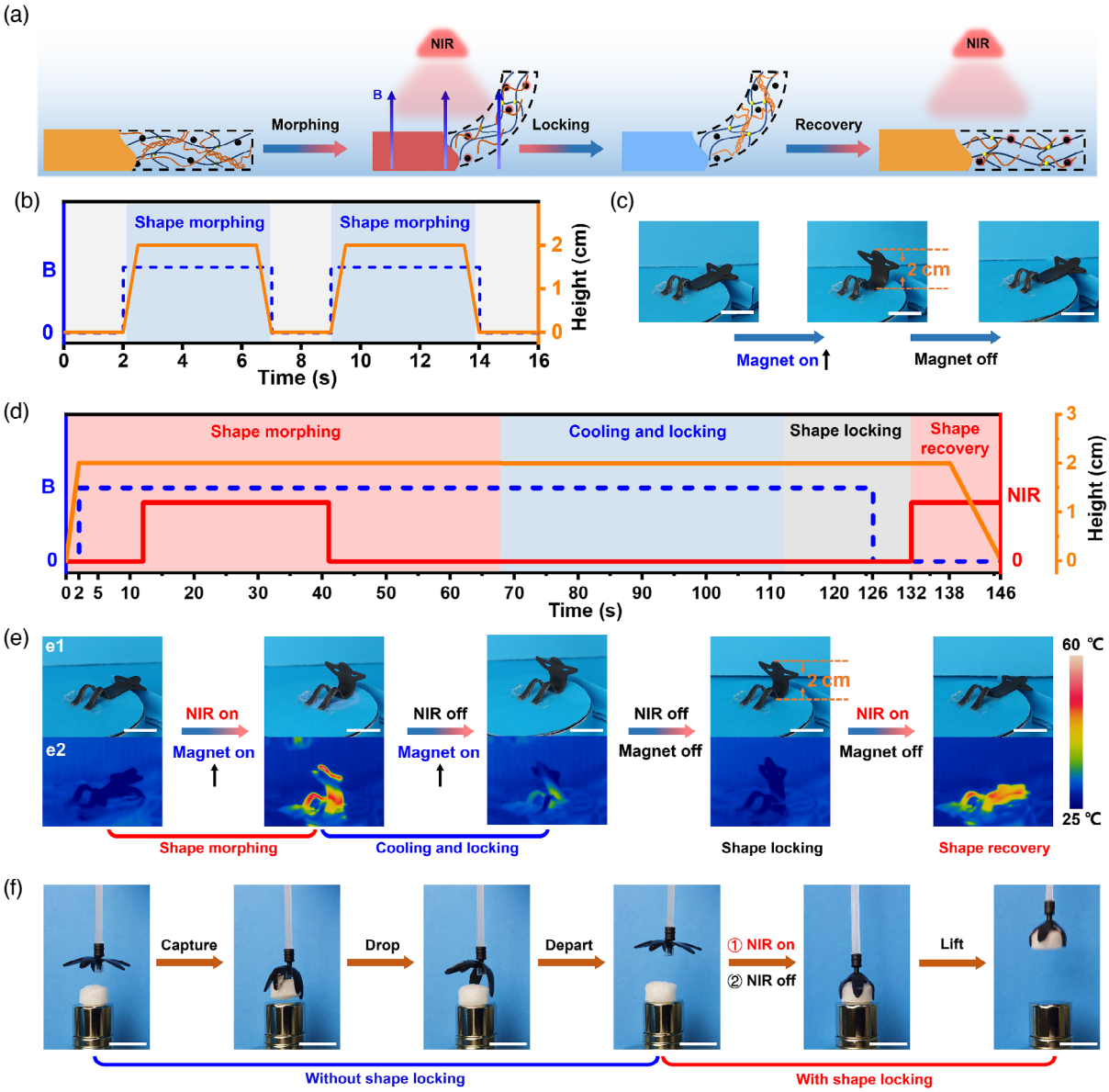

Figure 5. a) Schematic illustration of magnetic shape fixation and photothermal shape recovery process of HG-Fe_3O_4 hydrogel. b) The variation of the magnetic field and the sitting height of a hydrogel athlete with respect to time. c) The photos of the hydrogel athlete doing fast sit-ups with the assistance of magnetic field. d) The variation of the magnetic field, NIR light, and the sitting height of a hydrogel athlete with respect to time. e) The photos and infrared images of a hydrogel athlete doing sit-ups with the assistance of magnetic field and NIR light. f) A soft hydrogel gripper cannot pick up the object placed on a magnet without shape-locking process, and it can pick up the object after the folded shape is locked with the assistance of NIR light. Scale bars: 2 cm.

whether light is present or not. In the first mode, without NIR, a hydrogel athlete could be lifted quickly when a magnet approaches, and recovers to the flat gesture if the magnet is removed (Figure 5b,c and Movie S6, Supporting Information). In the second mode, with the NIR on, the hydrogel athlete could be lifted by a magnet; the magnet is kept for another 2 min after the NIR is switched off, the hydrogel athlete cools down and the sit-up position is locked. The sit-up gesture could be frozen for a long time, unless switching the NIR on; the gelatin network melts again and the robot could return to its initial flat position within 17 s. (Figure 5d,e and Movie S7, Supporting Information).

Soft grippers have many advantages; for instance, it is easy to deform and it will not destroy the grabbed object. Taking advantage of the magnetic shape fixation behavior, a soft hydrogel gripper that could pick up an object from a magnet was prepared (Figure 5f). An opened gripper is approached to an object that is placed on a magnet, and the open arms would fold and hold the object tightly due to the attraction of magnet. However, the object cannot be picked up because the soft gripper would open again once it is moved away from the magnet. With the assistance of the NIR light, the folded shape of the hydrogel gripper could be locked, and the object could be picked up (Movie S8, Supporting Information). Similarly, a hydrogel valve and a bird flutter model applying the same theory was also constructed (Figure S18, S19, Supporting Information).

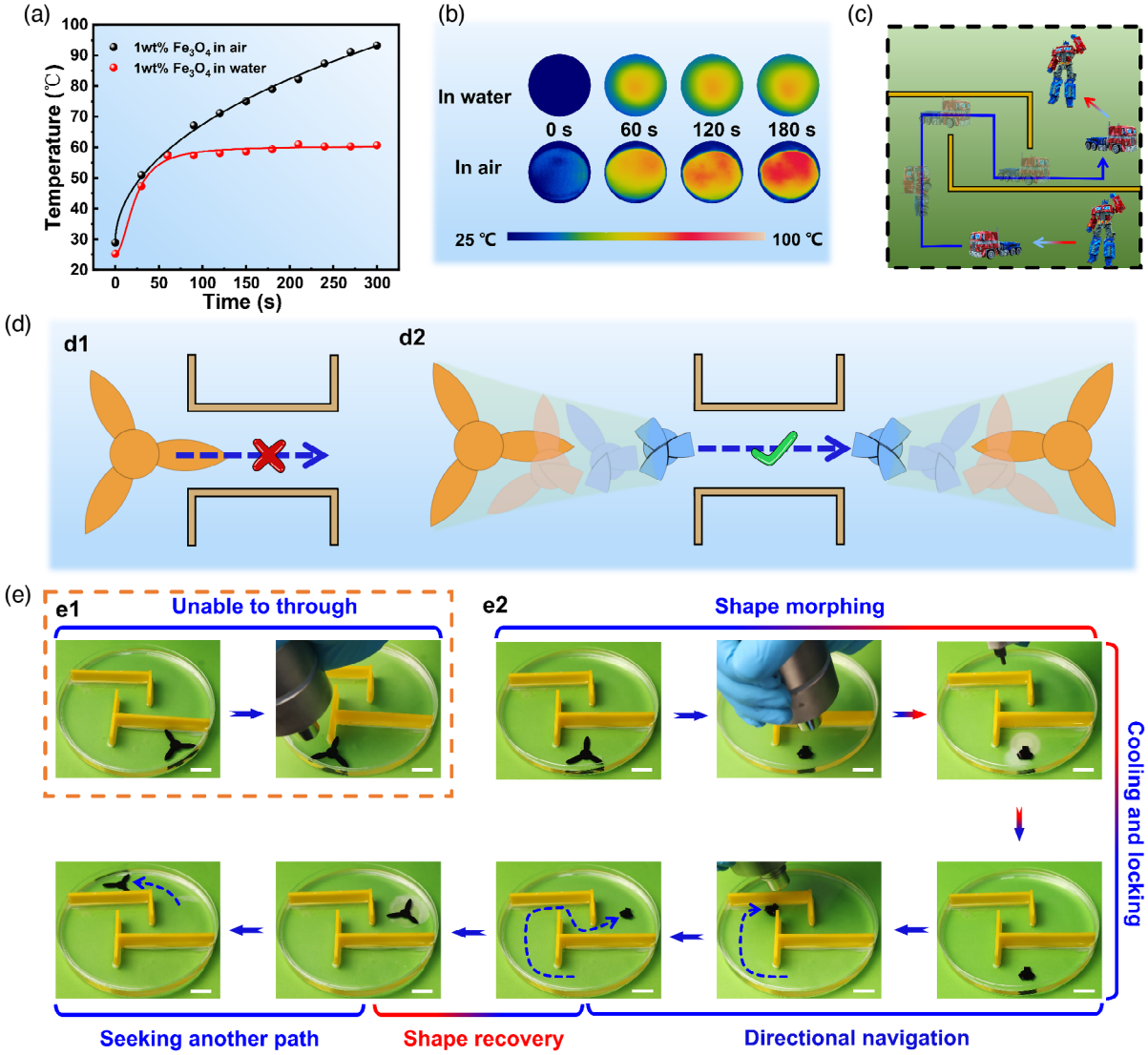

Figure 6. Magnetic directional navigation and photothermal shape recovery. a) The temperature increase of the HG-Fe_3O_4 hydrogel with 1 wt% Fe_3O_4 in water and air when illuminated by NIR. b) The infrared images of the HG-Fe_3O_4 hydrogel with 1 wt% Fe_3O_4 in water and air when illuminated by NIR for 0, 60, 120, 180 s. c) Schematic illustration of the directional navigation of Transformer and its shape-transformation process. d) The three-pawed soft Transformer cannot cross the narrow notches without shape morphing, and it can cross the narrow notches after the folded shape is locked with the assistance of magnetic field and NIR light. e) The images showing a three-pawed robot first deform into a folded shape, then navigate across a special maze guided by a magnet, and recovers to the unfolded shape when illuminated by NIR (Energy density is 3.06 W cm^{-2}). Scale bars: 2 cm.

2.5. Magnetically Directional Navigation and Photothermal Shape Recovery

Apart from the generation of temporary shape, the interaction between permanent magnet and Fe_3O_4 nanoparticles could be used to guide the HG-Fe_3O_4 hydrogel for directional navigation. Moreover, when exposed to NIR (3.06 W cm^{-2}), the temperature of a hydrogel disc could promptly rise to about 95 °C in air within 300 s (**Figure 6**a,b and Figure S20, Supporting Information). Even in water, the temperature of the hydrogel disc could increase to about 60 °C after irradiated by NIR for 60 s, which is higher than the melting temperature of gelatin. Therefore, NIR not only could induce shape recovery of the HG-Fe_3O_4 hydrogel in air but also could lead to the shape recovery in water.

It is well known that vehicles could choose the appropriate path guided by a global positioning system (GPS) navigation system (Figure 6c), as the HG-Fe_3O_4 hydrogel could be fixed into a smaller shape, which encourages us to combine magnet-induced directional navigation and photothermal shape memory to develop a soft Transformer across a maze. As shown in Figure 6d,e, a three-pawed robot with a diameter of 3.5 cm is prepared, and it is placed in a special maze filled with water; the robot is too large to navigate across the narrow channels of the maze. Because of its deformability, the soft robot could transform into a folded shape under the influence of a magnet, and the folded shape could be fixed with the assistance of NIR light. The folded robot is small enough to cross narrow notches, and finally reach a wide area, then NIR is applied to induce the shape recovery (Movie S9, Supporting Information). Moreover, a deformable soft carrier that is able to transport cargo through narrow passages, and release cargo at a particular position via shape recovery process have been fabricated (Figure S21, Movie S10, Supporting Information), which may have potential for a wide range of applications such as drug delivery and release.

3. Conclusion

In summary, we have presented a novel and effective strategy to construct soft hydrogel Transformers; magnetic and photothermal performances are intergrated into one SMH system; the obtained HG-Fe_3O_4 hydrogels have various advantages including noncontact shape deformation, self-healing, and directional navigation. The hydrogels are fabricated with a dual network structure which consists of a permanent PHEAA chemical network and a temporary gelatin physical network, and the shape memory property is achieved by the reversible sol–gel transition of gelatin. Fe_3O_4 magnetic nanoparticles are embedded in the hydrogel and endow the hydrogel with magnetic and photothermal response capabilities. In addition, the hydrogel also has good self-healing properties due to the coil-triple helix reversible transformation of gelatin. Combining the magnetic actuation and photothermal performance, noncontact shape manipulation and shape memory could be achieved both in water and in the air; a series of soft robots including soft gripper, hydrogel athlete, soft Transformer and hydrogel carrier have been constructed to demonstrate the magnetically driven transformation, and light-responsive shape memory and self-healing behaviors. We believe this design strategy will inspire the fabrication of novel intelligent systems with great potential in various fields.

Supporting Information

Supporting Information is available from the Wiley Online Library or from the author.

Acknowledgements

This work was supported by the National Key Research and Development Program of China (2018YFB1105100), National Natural Science Foundation of China (51873223, 52073295), Youth Innovation Promotion Association of Chinese Academy of Sciences (2017337), and Key Research Program of Frontier Science, Chinese Academy of Sciences (QYZDB-SSW-SLH036).

Conflict of Interest

The authors declare no conflict of interest.

Keywords

hydrogel transformers, magnetic manipulations, multi-field synergy, self-healing, shape memory hydrogels

Received: September 11, 2020
Revised: November 4, 2020
Published online: December 3, 2020

[1] A. Lendlein, O. E. C. Gould, *Nat. Rev. Mater.* **2019**, *4*, 116.
[2] Q. Zhao, H. J. Qi, T. Xie, *Prog. Polym. Sci.* **2015**, *49–50*, 79.
[3] D. Habault, H. J. Zhang, Y. Zhao, *Chem. Soc. Rev.* **2013**, *42*, 7244.
[4] W. Lu, X. X. Le, J. W. Zhang, Y. J. Huang, T. Chen, *Chem. Soc. Rev.* **2017**, *46*, 1284.
[5] Y. Zhang, H. Gao, H. Wang, Z. Xu, X. Chen, B. Liu, Y. Shi, Y. Lu, L. Wen, Y. Li, Z. Li, Y. Men, X. Feng, W. Liu, *Adv. Funct. Mater.* **2018**, *28*, 1705962.
[6] K. Wang, Y.-G. Jia, C. Zhao, X. X. Zhu, *Prog. Mater Sci.* **2019**, *105*, 100572.
[7] Y. Zhang, X. Le, Y. Jian, W. Lu, J. Zhang, T. Chen, *Adv. Funct. Mater.* **2019**, *29*, 1905514.
[8] S. Y. Zhuo, Z. G. Zhao, Z. X. Xie, Y. F. Hao, Y. C. Xu, T. Y. Zhao, H. J. Li, E. L. Knubben, L. Wen, L. Jiang, M. J. Liu, *Sci. Adv.* **2020**, *6*, 10.
[9] G. G. Zhang, W. J. Peng, J. J. Wu, Q. Zhao, T. Xie, *Nat. Commun.* **2018**, *9*, 4002.
[10] B. J. Jin, H. J. Song, R. Q. Jiang, J. Z. Song, Q. Zhao, T. Xie, *Sci. Adv.* **2018**, *4*, eaao3865.
[11] C. Lowenberg, M. Balk, C. Wischke, M. Behl, A. Lendlein, *Acc. Chem. Res.* **2017**, *50*, 723.
[12] Y. K. Jian, W. Lu, J. W. Zhang, T. Chen, *Acta Polym. Sin.* **2018**, *11*, 1385.
[13] H. Chen, Y. Li, G. Tao, L. Wang, S. Zhou, *Polym. Chem.* **2016**, *7*, 6637.
[14] X. B. Hu, M. Vatankhah-Varnoosfaderani, J. Zhou, Q. X. Li, S. S. Sheiko, *Adv. Mater.* **2015**, *27*, 6899.
[15] Y. N. Chen, L. F. Peng, T. Q. Liu, Y. X. Wang, S. J. Shi, H. L. Wang, *Acs Appl. Mater. Interfaces* **2016**, *8*, 27199.

[16] M. Pan, Q. J. Yuan, X. L. Gong, S. Zhang, B. J. Li, *Macromol. Rapid Commun.* **2016**, *37*, 433.
[17] K. Miyamae, M. Nakahata, Y. Takashima, A. Harada, *Angew. Chem. Int. Ed.* **2015**, *54*, 8984.
[18] L. Tang, S. Liao, J. Qu, *ACS Appl. Mater. Interfaces* **2019**, *11*, 26346.
[19] C. Zhao, P. Zhang, J. Zhou, S. Qi, Y. Yamauchi, R. Shi, R. Fang, Y. Ishida, S. Wang, A. P. Tomsia, M. Liu, L. Jiang, *Nature* **2020**, *580*, 210.
[20] J. Ban, L. Mu, J. Yang, S. Chen, H. Zhuo, *J. Mater. Chem. A* **2017**, *5*, 14514.
[21] X. Liu, J. Zhang, M. Fadeev, Z. Li, V. Wulf, H. Tian, I. Willner, *Chem. Sci.* **2019**, *10*, 1008.
[22] M. Xie, C. Wu, C. Chen, Y. Liu, C. Zhao, *Polym. Chem.* **2019**, *10*, 4852.
[23] C. Jiao, Y. Chen, T. Liu, X. Peng, Y. Zhao, J. Zhang, Y. Wu, H. Wang, *ACS Appl. Mater. Interfaces* **2018**, *10*, 32707.
[24] X. X. Le, W. Lu, H. Xiao, L. Wang, C. X. Ma, J. W. Zhang, Y. J. Huang, T. Chen, *Acs ACS Appl. Mater. Interfaces* **2017**, *9*, 9038.
[25] Z. G. Zhao, K. J. Zhang, Y. X. Liu, J. J. Zhou, M. J. Liu, *Adv. Mater.* **2017**, *29*, 8.
[26] A. Yasin, H. Z. Li, Z. Lu, S. U. Rehman, M. Siddiq, H. Y. Yang, *Soft Matter* **2014**, *10*, 972.
[27] T. T. Zhao, M. Tan, Y. L. Cui, C. Deng, H. Huang, M. Y. Guo, *Polym. Chem.* **2014**, *5*, 4965.
[28] Y. Zhang, J. Liao, T. Wang, W. Sun, Z. Tong, *Adv. Funct. Mater.* **2018**, *28*, 1707245.
[29] G. Li, Q. Yan, H. S. Xia, Y. Zhao, *ACS Appl. Mater. Interfaces* **2015**, *7*, 12067.
[30] F. Zhang, Y. Xia, L. Wang, L. Liu, Y. Liu, J. Leng, *ACS Appl. Mater. Interfaces* **2018**, *10*, 35526.
[31] L. Wang, Y. Jian, X. Le, W. Lu, C. Ma, J. Zhang, Y. Huang, C. F. Huang, T. Chen, *Chem. Commun.* **2018**, *54*, 1229.
[32] C. F. Dai, C. Du, Y. Xue, X. N. Zhang, S. Y. Zheng, K. Liu, Z. L. Wu, Q. Zheng, *ACS Appl. Mater. Interfaces* **2019**, *11*, 43631.
[33] H. Yang, W. R. Leow, T. Wang, J. Wang, J. Yu, K. He, D. Qi, C. Wan, X. Chen, *Adv. Mater.* **2017**, *29*, 1701627.
[34] J. H. Huang, L. Zhao, T. Wang, W. X. Sun, Z. Tong, *ACS Appl. Mater. Interfaces* **2016**, *8*, 12384.
[35] Q. Ze, X. Kuang, S. Wu, J. Wong, S. M. Montgomery, R. Zhang, J. M. Kovitz, F. Yang, H. J. Qi, R. Zhao, *Adv. Mater.* **2019**, *32*, 1906657.
[36] J. A.-C. Liu, J. H. Gillen, S. R. Mishra, B. A. Evans, J. B. Tracy, *Sci. Adv.* **2019**, *5*, eaaw2897.
[37] J. Tang, Q. Yin, Y. Qiao, T. Wang, *ACS. Appl. Mater. Interfaces* **2019**, *11*, 21194.
[38] F. Cuppo, M. Venuti, A. Cesàro, *J. Biol. Macromol.* **2001**, *28*, 331.
[39] L. Guo, R. H. Colby, C. P. Lusignan, T. H. Whitesides, *Macromolecules* **2003**, *36*, 9999.
[40] W. Nan, W. Wang, H. Gao, W. Liu, *Soft Matter* **2013**, *9*, 132.
[41] A. Lendlein, S. Kelch, *Angew. Chem. Int. Ed.* **2002**, *41*, 2034.
[42] X. Yan, Q. Chen, L. Zhu, H. Chen, D. Wei, F. Chen, Z. Tang, J. Yang, J. Zheng, *J Mater. Chem. B* **2017**, *5*, 7683.